II International Conference on Particle-based Methods – Fundamentals and Applications
PARTICLES 2011
E. Oñate and D.R.J. Owen (Eds)

DEM SIMULATION OF THE MECHANICAL PROPERTIES OF SiC CERAMIC UNDER PRE-STRESSING

S.Q. JIANG[*], Y.Q. TAN[*], H. ZHANG[*], D.M. YANG[*†] AND G.F. ZHANG[*]

[*] School of Mechanical Engineering
Xiangtan University, Xiangtan 411105, China
Email: jsqcx@126.com, tanyq@xtu.edu.cn

[†] School of Civil Engineering
University of Leeds, Leeds, LS2 9JT, UK
Email: cndy@leeds.ac.uk

Key words: DEM, Mechanical properties, SiC, Pre-stress.

Abstract. In this paper, the method of discrete element model (DEM) simulation was used to investigate the mechanical properties of SiC ceramic materials under the action of pre-stress. Using the bonded particle model (BPM), several different numerical tests (such as UCT, TPB, SENB tests) of SiC ceramic were established. Different pre-stress values were applied on the lateral surface of the ceramic specimen during the numerical simulation process, all tests were carried out at least 5 times with different random number, and the average mechanical properties results were calculated. It was showed that the existence of pre-stress has a significant effect on the mechanical properties of materials. It can enhance the strength of materials, while the force action on material in machining process force or action force the crack's initiation and propagation was limited.

1 INTRODUCTION

Special ceramic materials such as silicon carbon, silicon nitride, alumina and zirconia are considered to be used in sealing elements, bearings, cutting tools, engine components, wear-resistant coatings and other applications for their excellent properties. Usually, the applications of ceramic materials require the parts or components with high dimensional tolerances and good surface finish. However, the hardness and brittleness of materials make the machining processing very difficult and grinding becomes one of the main machining methods. The grinding quality of ceramic components is very difficult to control because the interaction between tool and ceramic surface in grinding process can cause material damages, e.g. surface/sub-surface cracks and residual stress [1, 2]. Those damages produced by machining can be detrimental to the strength and performance of components.

Until recently, many studies of damage have been conducted with the aim to reduce machining damage. Several novel grinding technology with the applications of additional physical or chemical actions have been proposed to obtain better machining efficiency and quality, such as electrolytic in-process dressing (ELID) [3], ion beam figuring (IBF) [4], magneto-rheological finishing (MRF) [5], etc. Inspired by these applications, we argue that application of external forces or stresses, which are used to change the stresses field within

the specimen before and during the machining process, may change the final material damage mechanism. Huang et al [6] studied the effects of lateral stress in indentation experiments of rock. They found that the lateral restraint stresses can change the damage zone of the indentation, and the transverse cracks can replace the median cracks to some extent. Head and Cline [7] studied several polycrystalline ceramics of high-restraint stress in quasi-static triaxial compression experiments and found the transition phenomenon of ceramics from brittle fracture to plastic behavior. Yoshino et al. [8] studied monocrystalline silicon under hydrostatic pressure in the scratching and single-point diamond cutting and found that there was a significant improvement in the damage and surface roughness. In our earlier study, we also found that the existence of pre-stress can restrain the crack propagation and the obvious plastic deformation can be found at the bottom of scratched groove [9, 10]. However, little attention has been devoted to how the external forces or stresses affecting on the materials mechanical properties, and from the viewpoint of mechanical properties of materials, the reasons why the existence of pre-stress can reduce the machining damages are still needed to be investigated.

The purpose of this paper is to investigate how the pre-stress affecting the materials mechanical properties by discrete element model (DEM) simulations. Several different numerical tests were carried out to get the mechanical properties of SiC ceramic under the action of different pre-stress values. The results in this paper may be used to explain why the existence of pre-stress can reduce the machining damages of materials and get better surface quality of components.

2 DISCRETE ELEMENT METHOD (DEM)

DEM was firstly introduced by Cundall [11] for analysis of rock-mechanics problems. It assumes that the small particles are circular in 2D or spherical in 3D and can overlap or detach. Essentially, DEM is not based on the continuum mechanics, which is the most difference between finite element method (FEM) and discrete element method. DEM can simulate the granular material with larger deformation as well as simulating the fracture behavior of solid brittle materials, such as geo-materials [12], concrete [13, 14], ceramic [15] etc. The calculations performed in the DEM alternate between the application of Newton's second law to the particles and a force-displacement law at the contacts. The motion equation of Newton's second law in the DEM can be described as following:

$$m_i \frac{dv_i}{dt} = \sum_{j=1}^{k_i} \left(F_{c,ij} + F_{d,ij} \right) + m_i g + F_i \tag{1}$$

Where m_i is the mass of particle i, v_i is its translational velocity and k_i is the number of particles in contact with i at time t. F_c is the contact force of particle i, F_d is the damping force of particle i, $m_i g$ is the gravitational force, F_i is the external force action on particle i.

According to force-displacement law, the resulting contact force acting on the contact between two particles can be described as following:

$$\vec{F} = F^n \vec{n} + F^s \vec{s} \tag{2}$$

Where $\vec{F}$ is the resulting force, F^n is the normal force and F^s is the shear force. The normal force and shear force can be calculated by

$$F^n = K^n U^n \tag{3}$$

$$F^s = F^s + \Delta F^s \tag{4}$$

$$\Delta F^s = -K^s \Delta U^s \tag{5}$$

Where K^n and K^s are the normal and shear components of the contact stiffness, U^n is the overlap between two contact particles, ΔU^s is the shear component of the displacement.

3 DEM SIMULATION

3.1 DEM modeling of SiC ceramic

In this paper we used the PFC2D [16] (particle flow codes in two dimensions) as the simulation platform. And the bonded-particle model (BPM) also was adopted, which can be envisioned as a kind of cemented with a finite size joining the two particles, as shown in Figure.1. A parallel bond can be regarded as a set of elastic springs with constant stiffness (normal and shear) and strength (tensile and shear), uniformly distributed over a rectangular cross-section lying on the contact plane and centered at the contact point. It can transmit both force and moment. If the maximum tensile stress exceeds the tensile strength or the maximum shear stress exceeds the shear strength, then the parallel bond breaks (represents an individual micro-crack).

Based on PFC2D, we use the specimen-genesis procedure from Augmented FishTank [16] to generate the sample of needed BPM model that is similar to the micro-structure of SiC. In order to represent the complex-shaped grains of SiC, we make a number of particles bonded into a cluster. The clustering algorithm is controlled by Sc, the maximum number of particles in a cluster. Each cluster is grown by identifying the current particle as a seed particle and then adding adjacent particles to the cluster until either all adjacent particles have been added or the cluster size has reached Sc. It can clearly to see that the algorithm provides no control over cluster shape but does produce a collection of complex cluster shapes that are extremely similar to the grains in a polycrystalline SiC ceramic. The results are shown in Figure.2. Here we set the maximum allowable number of particles in a cluster equal to 7, and different colors represent the different clusters.

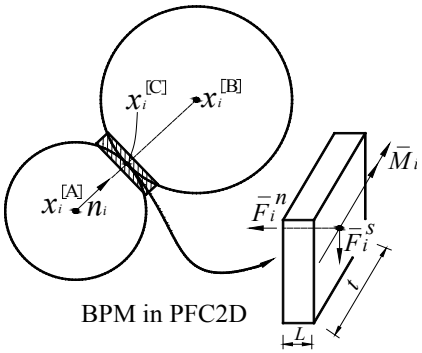

Figure.1 Sketch map of parallel bond.

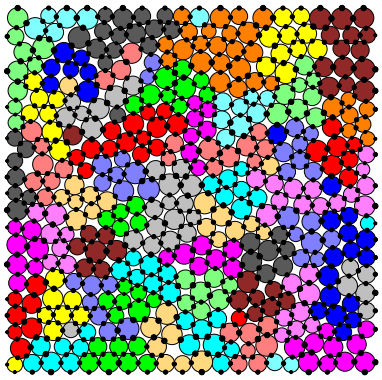

Figure.2 Complex-shaped grains of SiC material in PFC2D.

3.2 Calibration of the DEM model of SiC ceramic

In general sense, the macro-properties of ceramics are usually described by its elastic modulus, unconfined compressive strength, Poisson's ratio, bending strength and fracture

toughness etc., while for codes such as PFC that synthesize macro-properties material behavior from the interactions of micro-scale components, the input properties of the microscopic constituents are usually not known. In order to have a confidence that the particular model is reproducing desired physical behavior, it is necessary to calibration the micro-parameters of DEM model. To some extent, this is a trial and error process, because there is no complete theory that can predict macroscopic behavior form microscopic properties and geometry [16]. However, this can be achieved by several numerical experiments. In this paper, the distributions of particles were random in specified region, and the average radius of particles was 2 μm. The main mechanical properties which are Young's modulus, compressive strength, Poisson's ratio, fracture toughness and bending strength are simulated by uniaxial compressive test (UCT), three point bending test (TPB) and single edge notched bending test (SENB). The size of DEM model for UCT test was 0.3 mm × 0.8 mm, consisting of 2077 clusters and 10267 balls. The size of DEM model of TPB and SENB tests was 1.0 mm × 0.25 mm, consisting of 2077 clusters and 10267 balls. All of the numerical tests were simulated at least 5 times with different random numbers to eliminate the impact of random errors. The numerical results of mechanical properties with comparison of experimental measurements are presented in Table 1.

Table 1. The main mechanical properties of SiC in experiment tests and in 2D DEM simulations

Mechanical properties	Test results	DEM model
Young's modulus E [Gpa]	420	425.7
Poisson's ratio v	0.14	0.138
Uniaxial compressive strength [Mpa]	2000	2019.8
Bending strength [Mpa]	500-800	658.1
Fracture toughness [MPa/m$^{1/2}$]	3.5	3.54

3.3 DEM modeling of mechanical properties of SiC ceramic with pre-stress

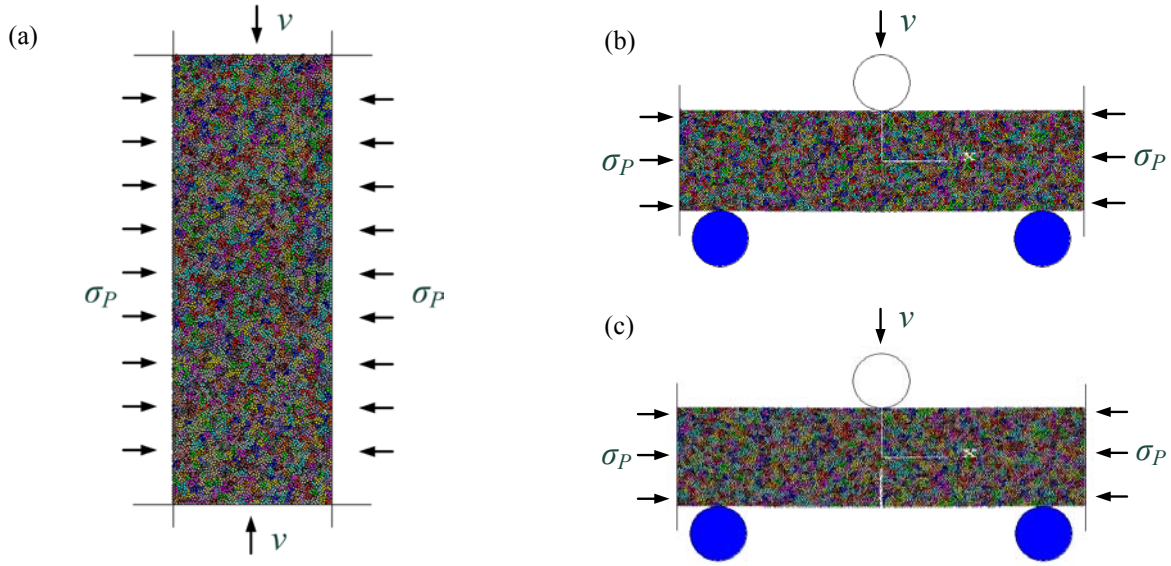

Figure.3 DEM model of mechanical behaviors under pre-stress, (a) UCT; (b) TPB; (c) SENB

In order to investigate the effect of pre-stress on mechanical properties of SiC ceramic, different pre-stress values (0, 50, 100, 200, 300 and 400 MPa) were applied on the lateral surface of the ceramic specimen during the numerical simulation process, as shown in

Figure.3. Similarly, the numerical tests under different pre-stresses were carried out five times by changing the random number in the models. During the UCT test, the loading speed (top and bottom walls act as loading platens) is specified as 0.2 m/s, stress and strain acting throughout specimen are monitored using either wall-derived quantities or by using the stress and accumulated strains from measurement circles. The elastic modulus, unconfined compressive strength and Poisson's ratio are calculated by the axial stress-strain curves. During the TPB test and SENB test, the loading wall is specified as 0.05 m/s, the force in Y direction is recorded automatic. The bending strength and fracture toughness are calculated according to the peak force and specimen size.

4 RESULTS AND DISCUSSION

4.1 Failure response

Figure.4 shows the axial stress-strain curves under different pre-stress values. It can be clearly to see that brittle fracture is still the main material failure mode even if under the action of pre-stress. As the increasing of pre-stress, the peak stress is also increased. However, there is a little changing in the slopes of the axial stress-strain curves under different pre-stresses. As shown in Figure.5, the Y direction force in TPB test and SENB test are increased as the increasing of pre-stress. When the applied pre-stress is 400 MPa, the peak force for both TPB and SENB test has reached 100 kN. The higher the force acting on the specimen indicates that the bending strength and fracture toughness is greater.

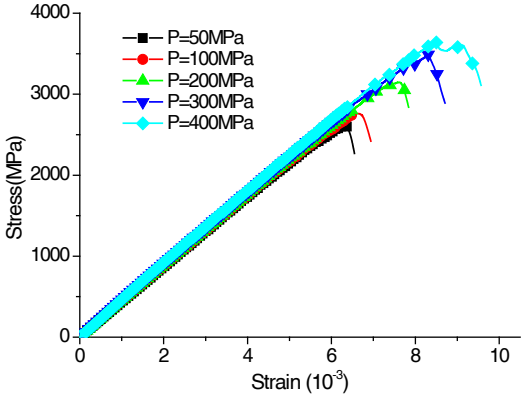

Figure.4 Axial stress versus axial strain for SiC ceramic under different pre-stress values.

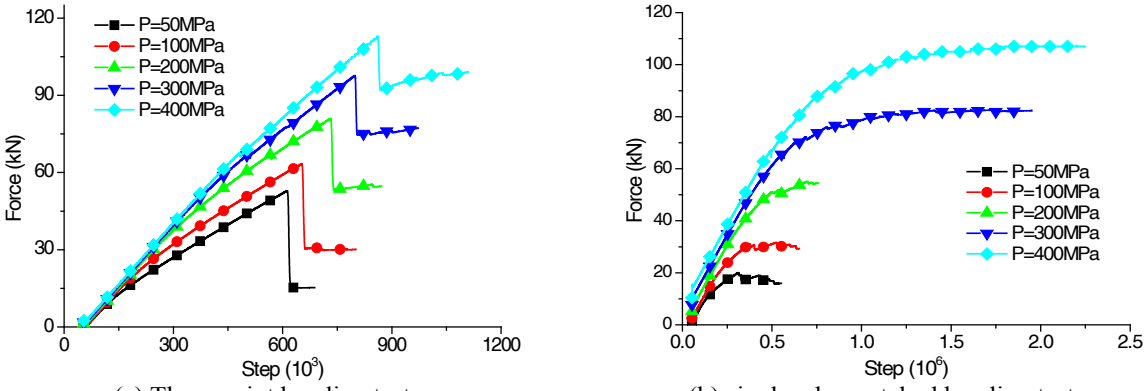

(a) Three point bending test (b) single edge notched bending test

Figure.5 Force versus steps of TPB test and SENB test for SiC ceramic under different pre-stress values.

4.2 Mechanical properties

According to the previously mentioned failure analysis, the mechanical properties of SiC ceramic are calculated. The averages of mechanical properties are also calculated, as shown in Figure.6. It is found that the existence of pre-stress affect the mechanical properties of SiC ceramic obviously. As the increasing of pre-stress, the Poisson's ratio of SiC ceramic was deceased, and the Young's modulus, compressive strength, fracture toughness and bending strength were increased monotonically. That is to say, the existence of pre-stress make the SiC ceramics has enhanced strength, stiffness, and its deformability reduced. The materials under pre-stressing showed that a part of mechanical properties of ceramics make it become harder, more brittle and more strength, just like a "super-ceramic".

The existence of pre-stress enhanced the strength and stiffness of ceramic when the pre-stress was applied on the lateral surface of materials. According to our previous studies [9, 17], the existence of pre-stress has a little effect on scratching tangential force or cutting force. It is shown that the cutting force action on the materials almost keeps the same, while the material's strength under pre-stress was enhanced, so it can resist or limit the crack's initiation and propagation. However, the existence of pre-stress did not increase the deformability of ceramic materials. In addition, from the results of axial stress-strain curves, it can be seen that the failure mode of ceramic under pre-stress was main brittle fracture.

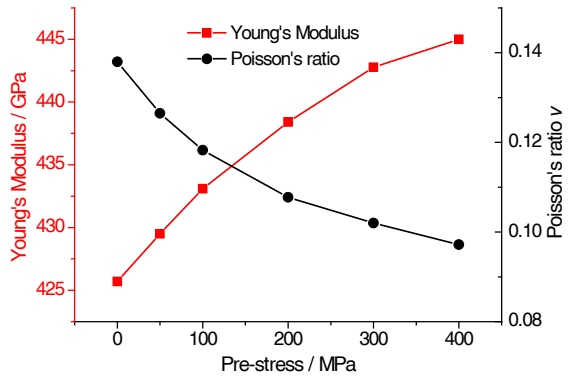

(a) Young's modulus and Poisson's ratio

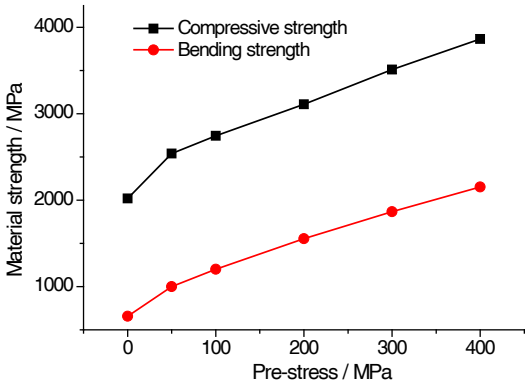

(b) Compressive strength and bending strength

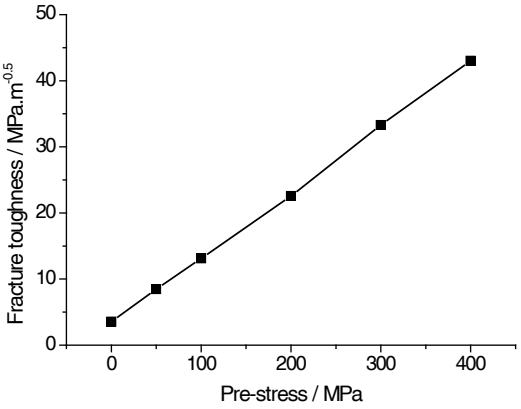

(c) Fracture toughness

Figure.6 Effects of pre-stress on mechanical properties of SiC ceramic.

5 CONCLUSIONS

- According to UCT results with different pre-stress values, brittle fracture is still the main material failure mode.
- The existence of pre-stress has a significant effect on the mechanical properties of materials. As the increasing of pre-stress, the Poisson's ratio of SiC ceramic was deceased, and the Young's modulus, compressive strength, fracture toughness and bending strength were increased monotonically.
- The existence of pre-stress enhanced the strength of materials, so it can resist or limit the crack's initiation and propagation.

ACKNOWLEDGEMENT

This research work was supported by the National Natural Science Foundation of China (50875224) and the Hunan Provincial Innovation Foundation for Postgraduate (CX2010B262).

REFERENCES

[1] Hessert, R., Eigenmann, B., Vöhringer, O. and Löhe, D. Fracture mechanical evaluation of the effects of grinding residual stresses on bending strength of ceramics. *Mater. Sci. Eng. A* (1997) 234-236: 1126- 1129.

[2] Yin, L., Vancoille, E.Y.J., Lee, L.C., Huang, H., Ramesh, K. and Liu, X.D. High-quality grinding of polycrystalline silicon carbide spherical surfaces. *Wear* (2004) 256: 197-207.

[3] Bandyopadhyay, B.P., Ohmori H. and Takahashi I. Efficient and stable grinding of ceramics by electrolytic in-process dressing (ELID). *J. Mater. Process. Tech.* (1997) 66:18-24.

[4] Allen, D.M., Shore, P., Evans, R.W., Fanara, C., O'Brien, W., Marson S. and O'Neill W. Ion beam, focused ion beam, and plasma discharge machining. *CIRP Ann.-Manuf. Tech.* (2009) 58: 647-662.

[5] Zhang, F.H., Kang, G.W., Qiu Z.J. and Dong, S. Magnetorheological finishing of glass ceramic. *Key Eng. Mat.* (2004) 257-258: 511-514.

[6] Huang, H., Damjanac, B. and Detournay, E. Numerical modeling of normal wedge indentation rocks with lateral confinement, *Int. J. Rock Mech. Min.* (1997) 34: 1023-1033.

[7] Head, H.C. and Cline C.F. Mechanical behavior of polycrystalline BeO, Al_2O_3 and AlN at high pressure. *J. Mater. Sci.* (1980) 15: 1889-1897.

[8] Yoshino, M. and Ogawa, Y. Machining of hard-brittle material by a single point tool under external hydrostatic pressure. *J. Manuf. Sci. Eng.* (2005) 127: 837-845.

[9] Tan, Y.Q., Jiang, S.Q., Yang, D.M. and Sheng, Y. Scratching of Al_2O_3 under pre-stressing. *J. Mater. Process. Tech.* (2011) 211: 1217-1223.

[10] Jiang, S.Q., Tan Y.Q., Nie S.J., Peng, R.T., Yang D.M. and Li, G.R. Discrete element method (DEM) simulation and investigation of SiC on pre-stressed machining. *J. Inorg. Mater.* (2010) 25: 1286-1290.

[11] Cundall, P.A. and Strack, O.D.L. A discrete numerical model for granularassembles. *Geotechnique*. (1979) 29: 47-65.

[12] Hunt, S.P., Meyers, A.G. and Louchnikov, V. Modelling the Kaiser effect and deformation rate analysis in sandstone using the discrete element method. *Comput.*

Geotech. (2006) 30: 611–621.
[13] Frédéric, S.H., Donzé, V. and Daudeville, L. Discrete element modeling of concrete submitted to dynamic loading at high strain rates. *Comput. Struct.* (2004) 82: 2509–2524.
[14] Shiu, W.J., Donze, F.V. and Daudeville, L. Compaction process in concrete during missile impact: a DEM analysis. *Comput. Concrete* (2008) 5:329–342.
[15] Tan, Y.Q, Yang, D.M. and Sheng, Y. Study of polycrystalline Al_2O_3 machining cracks using discrete element method. *Int. J. Mach. Tool. Manu.* (2008) 48: 975-982.
[16] Itasca Consulting Group Inc., PFC2D (particle flow code in 2-dimensions), Version 3.10, Minneapolis, Minnesota, 2004.
[17] Jiang, S.Q., Tan, Y.Q., Yang, D.M. and Sheng, Y. Study on cutting forces of SiC machining process with pre-stressed using DEM simulation. The Fifth International Conference on Discrete Element Methods, London, 2010.